Carbocatalytic dehydration of xylose to furfural in water

Lam, Edmond; Chong, Jonathan H.; Majid, Ehsan; Liu, Yali; Hrapovic, Sabahudin; Leung, Alfred C. W.; Luong, John H. T.

Publisher's version / Version de l'éditeur:
https://doi.org/10.1016/j.carbon.2011.10.007
Carbon, 50, 3, pp. 1033-1043, 2011-10-12

CARBON 50 (2012) 1033–1043

Available at www.sciencedirect.com

SciVerse ScienceDirect

journal homepage: www.elsevier.com/locate/carbon

Carbocatalytic dehydration of xylose to furfural in water

Edmond Lam, Jonathan H. Chong, Ehsan Majid, Yali Liu, Sabahudin Hrapovic, Alfred C.W. Leung, John H.T. Luong *

Biotechnology Research Institute, National Research Council Canada, 6100 Royalmount Avenue, Montreal, Quebec, Canada H4P 2R2

ARTICLE INFO

Article history:
Received 15 August 2011
Accepted 4 October 2011
Available online 12 October 2011

ABSTRACT

Graphene, graphene oxide, sulfonated graphene, and sulfonated graphene oxide (SGO) have been prepared, characterized and tested for the dehydration of xylose to furfural in water. In particular, SGO was proven to be a rapid and water-tolerant solid acid catalyst even at very low catalyst loadings down to 0.5 wt.% vs xylose, maintaining its initial activity after 12 tested repetitions at 200 °C, with an average yield of 61% in comparison to 44% for the uncatalyzed system. Raman spectroscopy, energy dispersive X-ray spectroscopy, thermogravimetric analysis, X-ray photoelectron spectroscopy, ^{13}C solid state nuclear magnetic resonance spectroscopy, Fourier transform infrared spectroscopy and surface area analysis suggested that the aryl sulfonic acid groups were the key active sites for high temperature production of furfural in water. They were more thermally stable under the reaction conditions and acidic than other functional groups attached to the graphene surface.

1. Introduction

Furfural derived from hemicellulose has been considered as a sustainable intermediate for the preparation of fine chemicals, pharmaceuticals, and furan-based polymers [1,2]. Acid hydrolysis is capable of hydrolyzing hemicellulosics to xylose, followed by the dehydration of the latter to form furfural in only 40–50% yield (Fig. 1) [1]. Use of solid acids such as zeolites [3–5], heteropolyacids [6], and sulfonic acid functionalized-Mobil Catalytic Materials (MCMs) [7] with strong Brönsted acidity, high surface area and thermal stability have been attempted. Nafion, a sulfonated tetrafluoroethylene-based fluoropolymer-copolymer [8], has also been proven as an effective and reusable catalyst for the conversion of xylose to furfural [9]. However, these solid acid catalysts use organic solvents such as dimethyl sulfoxide and toluene which adds complexity to the large scale processing and isolation of furfural. In water, such catalysts often lose their activity due to poisoning of acidic sites by water [10]. For example, using MCM-41-SO_3H only achieves a 27% yield after 24 h at 140 °C in water (3% xylose solution, 66% catalyst wt. loading vs xylose), compared to 75% yield in DMSO [7].

Reactions in water to produce furfural are often carried out at higher temperatures using common soluble acids such as sulfuric acid and formic acid at 200 °C with yields of ~60% [11,12]. The addition of intermediate-stabilizing anions can increase the yield up to 80% [13,14]. However, the use of homogenous acid catalysts necessitates the handling of highly corrosive chemicals and requires the neutralization of acidic wastes prior to their disposal. Therefore, our aim of the work in this paper was to develop an economical catalyst with high thermal stability for the dehydration of xylose to furfural in water. The reusability of the catalyst reduces potential costs associated with capital investment, catalyst production, catalyst handling and waste disposal.

Recent reports have shown that carbonaceous materials are effective solid acid catalysts due to their high thermal stability, high chemical activity and low production costs [15–17]. Often these "carbocatalysts" are prepared by carbonization of sugar molecules in acid to form sulfonate-functionalized carbon particles. Sulfonated graphene (SG) has also been

* *Corresponding author:* Fax: +1 514 496 6265.
E-mail address: john.luong@cnrc-nrc.gc.ca (J.H.T. Luong).
0008-6223/$ - see front matter
doi:10.1016/j.carbon.2011.10.007

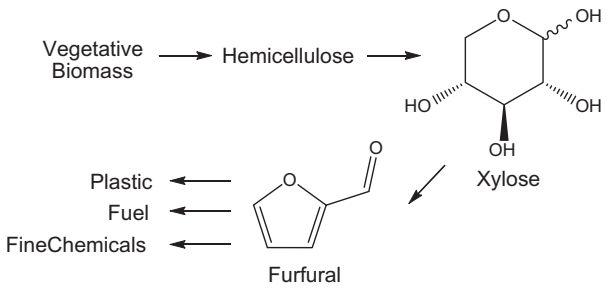

Fig. 1 – Conversion of hemicellulosic materials to xylose and then furfural.

demonstrated as a water-stable catalyst for the hydrolysis of ethyl acetate [18]. This study demonstrates the catalytic performance and reusability of graphene and its derivatives for the synthesis of furfural from xylose in aqueous solutions. In particular, sulfonated graphene oxide (SGO) will be demonstrated as a robust and reusable catalyst for repeated dehydration without losing its initial catalytic activity. Although carboxylic acid and sulfonic acid groups are present in SGO and are potentially active sites for xylose dehydration to occur, systematic analysis of the used catalyst suggests that the more thermally stable sulfonic acid groups are the key active acidic sites for high temperature production of furfural in water.

2. Experimental

2.1. Materials

D-(+)-Xylose, graphite powder, sulfuric acid, potassium persulfate, phosphorus pentaoxide, potassium permanganate, hydrogen peroxide (30%), hydrazine, sodium borohydride, sodium carbonate, sulfanilic acid, sodium nitrite, furfural, phloroglucinol (Sigma–Aldrich), graphene nanoplatelets (Cheaptubes.com), acetonitrile (J.T. Baker), hydrochloric acid (Fisher), and glacial acetic acid (EMD) were used as received.

2.2. Synthesis of graphene derivatives

Graphene oxide (GO) was synthesized using the modified Hummers' method [19] as described by Kovtyukhova et al. [20]. Graphite powder (20 g) was added to a solution of H_2SO_4 (30 mL), $K_2S_2O_8$ (10 g), and P_2O_5 (10 g) and heated at 80 °C for 2 h. The resulting black-blue suspension was filtered and washed with deionized water. The pre-oxidized graphite (10 g) was then added to ice-cold H_2SO_4 (230 mL). $KMnO_4$ (30 g) was added slowly to the solution with the temperature maintained at 35 °C for 2 h. The acidic graphite solution was slowly poured into a solution of 30% H_2O_2 (25 mL) in water (410 mL). The resultant brown solution was washed with 10% HCl solution and centrifuged three times at 10,000 rpm for 20 min. The resultant brown residue was dialyzed over deionized water and freeze-dried to give 17 g of GO.

SGO was prepared by Samulski's method [21]. GO (750 mg) was dispersed in water (750 mL) by sonication. A solution of $NaBH_4$ (6 g) in water (150 mL) was added dropwise to the GO dispersion, with the pH adjusted to 9.1 by addition of 5 wt.% Na_2CO_3 solution. The mixture was heated at 80 °C for 1 h, in which the brown GO turned black. The mixture was washed with water and centrifuged three times at 10,000 rpm for 20 min. The partially reduced GO was re-dispersed in water (750 mL) by sonication and cooled in an ice bath. A diazonium salt solution was prepared by adding sulfanilic acid (460 mg) to an ice-cold solution of 1 N HCl (5 mL) and water (100 mL) followed by the addition of $NaNO_2$ (180 mg) until all reactants had dissolved. The diazonium solution was poured into the ice-cold GO solution and stirred overnight. The black solution was washed with deionized water and centrifuged three times at 10,000 rpm for 20 min. The resultant black residue was dialyzed over deionized water and freeze-dried to give 450 mg of SGO.

SG was also prepared by Samulski's method [21]. SGO (200 mg) was dispersed in water (200 mL) by sonication. Hydrazine (2 mL) was added to the SGO suspension and heated for 24 h at 100 °C with constant stirring. The black solution was washed with deionized water and centrifuged three times at 10,000 rpm for 20 min. The resultant black residue was dialyzed over deionized water and freeze-dried to give 91 mg of SG.

2.3. Characterization

Scanning electron microscopy-energy dispersive X-ray (SEM-EDX) analysis was performed on a Hitachi S 2600N SEM (Hitachi Scientific Instruments, Tokyo, Japan) equipped with a microanalysis detector for EDX (Inca x-act, Oxford Analytical Instruments, Abington, UK). EDX spectra were collected at 30° angle, 20 kV accelerating voltage and a 20 nm working distance. EDX results were analyzed using incorporated Inca, Point and Analyze software. Low voltage transmission electron micrographs were obtained by a Delong LVEM (Soquelec, Montreal, QC, Canada) low-voltage TEM at 5 kV. A small amount of graphene material was suspended in water and sonicated to disperse the material. A 20 μL drop of well dispersed suspension was then dried on a Formvar-carbon coated grid and analyzed. Fourier transform infrared (FTIR) spectra were collected from graphene samples in KBr pellets at 4000–400 cm^{-1} for 64 scans at a resolution of 4 cm^{-1} using a Bruker Tensor 27 FTIR spectrophotometer. Raman spectra were acquired by a Horiba/Jobin-Yvon microconfocal Raman Analyzer (LabRAM HR 800, Horiba/Jobin-Yvon, Longjumeau, France) equipped with an argon-ion 514.5-nm laser operating at 200 mW. Raw data were smoothed using the standard smoothing function in the software and ASCII data were exported from the Labspec software into Microsoft Excel. Thermogravimetric analysis (TGA) was conducted with a Netzsch STA 449F1 instrument at a heating rate of 10 °C/min from room temperature to 800 °C under He purge gas. Catalytic acid sites of graphene and its derivatives were determined by titration [22]. XPS spectra were recorded in UHV ($<10^{-8}$ Torr) with an Axis Ultra DLD (Kratos Analytical Ltd.) utilizing a monochromatic Al KR source (1486.6 eV) and an analyzer pass energy of 160 eV for the survey and 20 eV for the high resolution scans. The analysis area (700 μm × 300 μm) was defined by an aperture in the transfer lens column. Charge neutralization current was applied. The binding energy was

referenced to graphene (284.5 eV). Peak fitting and quantification analysis were performed using the software package CasaXPS. The ^{13}C MAS NMR spectra were obtained using a Varian/Agilent VNMRS-400. Samples were placed in 4 mm zirconia rotors and spun at 10 kHz. In each case, 3000 transients were collected after 90° pulses with a recycle time of 5 s. Surface area measurements were performed using an adapted procedure for 1-naphthol adsorption [23].

2.4. *Catalytic conversion of xylose to furfural*

Batch catalytic experiments were performed in a mechanically stirred 5115 Parr Low Pressure reactor equipped with a 160 mL titanium vessel and a sampling port, and heated by an electronically controlled heating mantle. D-Xylose (2.25 g) and catalyst (45 mg) in water (75 mL) was added into the titanium vessel and sealed. The mixture was stirred at 300 rpm and heated from room temperature to the target temperature over 20 min. Zero time was taken to be the instant the internal temperature of the titanium vessel reached the target temperature. Samples were taken every 5 min from the sample port. The samples were cooled to room temperature and analyzed for furfural and unreacted xylose by HPLC.

2.5. *Analysis of xylose and furfural concentrations*

Furfural and xylose concentrations were determined by HPLC at 25 °C using a Shimadzu LCMS-2020. For furfural, a Shimadzu SPD-20A UV–Vis detector was set at 250 nm with an Ascentis C18 (#581324-U) 5 μm column. An acetonitrile/water (10:90 v/v) mixture was used as the mobile phase at 2.0 mL/min. Unreacted xylose content was separated using a Supelcosil LC-NH2 (#58338) 5 μm column and detected by a Shimadzu RID-10A refractive index detector. An acetonitrile/water (75:25 v/v) mixture was used as the mobile phase at 1.0 mL/min. The furfural and xylose concentrations were calculated from a calibration curve. Xylose conversion and furfural selectivity [24] were calculated as:

$$Conversion = \frac{mol\ of\ initial\ xylose - mol\ of\ unreacted\ xylose}{mol\ of\ initial\ xylose} \quad (1)$$

$$Selectivity = \frac{mol\ of\ furfural\ produced}{mol\ of\ initial\ xylose - mol\ of\ unreacted\ xylose} \quad (2)$$

3. Results and discussion

SEM revealed that pristine graphene nanoplatelets exhibited a single platelet structure while GO, SGO and SG adopted a more crumpled, layered structure (Fig. 2). EDX spectroscopy further confirmed that pristine graphene possessed the highest percentage of carbon and only 8% oxygen (Table 1). The oxidation of graphite to GO breaks up the sp^2-hybridized structure of the stacked graphene sheets with the basal plane decorated with hydroxyl and epoxy (1,2-ether) groups [25,26] GO had the largest percentage of oxygen (34%), due to the presence of oxygen-bearing functionalities. When GO was converted to SGO by pre-reduction of GO with $NaBH_4$ and covalent anchoring of aryl SO_3H groups to the graphene sheet, a corresponding decrease in oxygen was observed, ~28%. The reduction of SGO with hydrazine further lowered the oxygen content of SG to 18%.

GO had the highest ion exchange capacity (IEC) value of 2.0 meq H^+/g compared to 0.5 meq H^+/g for SG (Table 1). After the hydrazine treatment, the number of COOH groups may have decreased, as attested by the decrease in oxygen content. In all four cases, the materials exhibited sheet-like appearances in their TEM images, despite the presence of oxygen-bearing and SO_3H functional groups that might disrupt the sp^2 carbon network in GO, SGO and SG (Fig. 3).

FTIR spectra of the different materials were obtained to confirm the presence of different functional groups on the graphene sheet (Fig. 4). The spectrum of graphene is virtually featureless with the exception of the 1632 cm^{-1} peak associated with the skeletal vibrations of the graphitic sheet [27]. After graphite powder was oxidized, the spectrum of GO shows peaks at 1728 cm^{-1} ($\nu_{C=O}$), 1384 cm^{-1} (ν_{C-OH}), 1273 cm^{-1} (ν_{C-O-C}), and 1061 cm^{-1} (ν_{C-O}), for the carbonyl, hydroxyl, and epoxide groups, respectively [21]. After pre-reduction and sulfonation of GO to give SGO, peaks at 1171 cm^{-1} (ν_{S-O}), 1115 cm^{-1} (ν_{S-O}), and 1035 cm^{-1} ($\nu_{S-Phenyl}$) confirmed the presence of aryl SO_3H groups covalently bonded to the graphene sheet. The characteristic peaks at 1163 cm^{-1} (ν_{S-O}), 1115 cm^{-1} (ν_{S-O}), and 1033 cm^{-1} ($\nu_{S-Phenyl}$) for the aryl SO_3H groups were still present after further reduction of SGO with hydrazine, but peaks for the carbonyl groups were no longer visible. The loss of COOH groups through reduction might lead to a reduction in the IEC value and oxygen content by EDX as shown in Table 1 for SG.

Raman spectra and characterization data are presented in Table 1 and Fig. 5. For graphene, the Raman bands at 1348 cm^{-1} and 1569 cm^{-1} correspond to the D and G bands, respectively [28]. Blue shifts were observed for the G band in GO, SGO and SG, consistent with chemical doping of the graphene sheet [29]. The peak area ratio of the D and G bands (I_D/I_G) could be used to evaluate changes in the structure of the graphene sheet. Pristine graphene had a ratio of 0.06 while the other three materials had ratios that ranged from 0.78 to 1.16. The disruption of the sp^2 carbon network by functionalizing with COOH, epoxide, hydroxyl and aryl SO_3H groups contributes significantly to the intensity change in the D band [18].

^{13}C MAS NMR was performed to further examine the chemical reactions involved in the synthesis from GO to SG (Fig. 6A–C). During the oxidation process, the hydrophilic surface functional groups, such as epoxide, hydroxy, and carboxy groups will decorate the basal plane and the edge of graphene oxide [30]. As expected for GO, unoxidized sp^2 carbons appear at a chemical shift of 131 ppm. Carbon atoms associated with epoxide (61 ppm), hydroxyl (70 ppm) and carbonyl (165 ppm) groups are present in the spectrum [21,31–33]. For GO pre-reduction with $NaBH^4$ followed by sulfonation, the peak for the sp^2 carbons in SGO shifted down to 124 ppm. The peaks formerly at 61 and 165 ppm diminished, although the C–OH peak of 71 ppm remained unchanged. A small shoulder peak at 140 ppm confirmed the presence of carbon atoms bound to the phenyl–SO^3H groups. Finally, when SGO was reduced to SG with hydrazine, two key peaks were present in the SG spectra: sp^2 carbons (124 ppm) and the carbons bound to phenyl–SO^3H groups, present as a shoulder at 140 ppm.

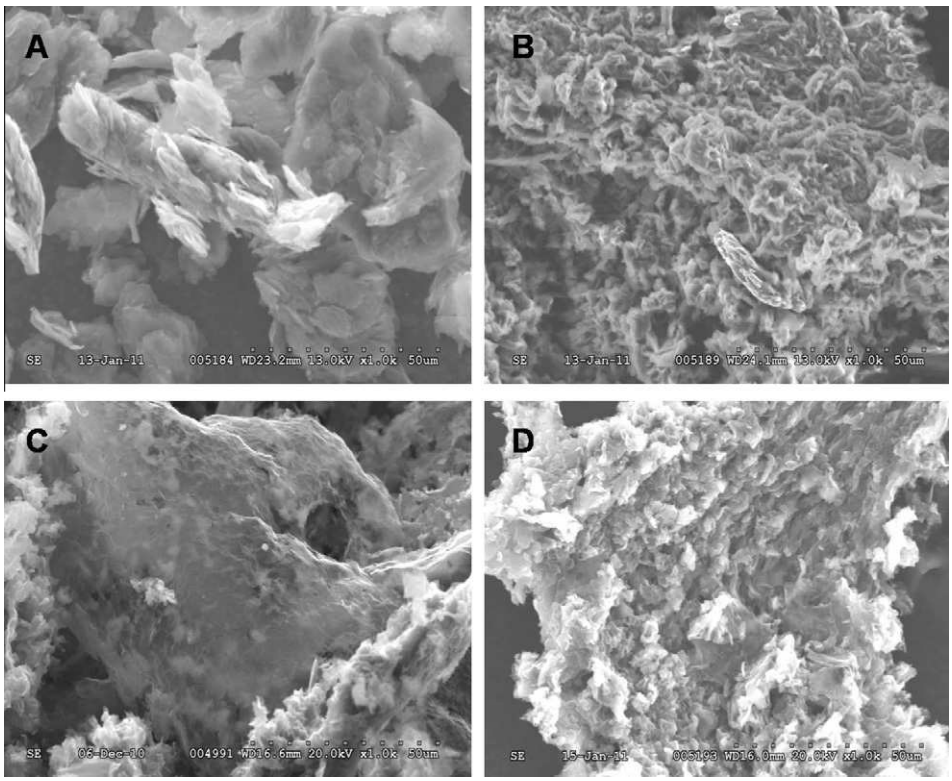

Fig. 2 – SEM images of (A) graphene, (B) GO, (C) SGO and (D) SG.

Table 1 – Characterization data for graphene and its derivatives.

Catalyst	IEC[a]	Surface area (m^2/g)	Elemental composition (%)			Raman bands (cm^{-1})		
			C	O	S	D	G	I_D/I_G[b]
Graphene	0.2	128	91.9	8.0	0.1	1348	1569	0.06
GO	2.0	318	65.4	34.0	0.6	1355	1591	1.16
SGO	1.7	680	71.9	27.6	0.6	1352	1583	1.27
SG	0.5	634	81.1	18.2	0.6	1357	1589	0.78

[a] meq H^+/g.
[b] Peak area ratio.

X-ray photoelectron spectroscopy (XPS) was also used to further analyze the elemental compositions from SGO to SG (Table 2). With each successive reduction step from GO to SG, the oxygen content decreased, consistent with the EDX data presented in Table 1.

Fig. 7 (top) shows the high resolution XPS spectrum for SGO with peaks for C 1s (283 eV), O 1s (530 eV) and S 2p (166 eV). The S 2p peak confirms the presence of phenyl–SO_3H groups. Together with ^{13}C MAS NMR information, peak deconvolution of the high resolution XPS spectrum (Fig. 7, bottom) confirmed that the C 1s peak consisted of four different oxygen bearing functional groups: sp^2 carbon (284.5 eV), C–O (286.6 eV), C=O (287.9 eV), and O–C=O (289.0 eV). Also present in the spectrum is the π to π^* transition (shake-up) at around 290.5 eV. Such results revealed that the most abundant of the oxygen-bearing functionalities in SGO were hydroxyl groups.

The catalytic activity of graphene and its derivatives for the dehydration of xylose to furfural was examined (see Table 3). Without any catalyst a furfural yield of 44% was achieved. It was reasoned that high temperature liquid water acted as an acid due to its tendency to self-ionize in comparison to ambient temperature water [34]. SGO achieved a peak yield of 62% at 200 °C in 35 min at 2% catalyst wt. loading vs xylose. In comparison, a peak yield of 46% furfural yield was reported for an aqueous xylose solution catalyzed by zeolite ZSM-5 at 200 °C in 16 min (10% xylose aqueous solution, 30% catalyst wt. loading vs xylose) [5].

Carbonaceous materials are attractive materials for catalysts due to their high surface area which may provide adequate catalytic active sites. To investigate whether surface area plays an integral role in the higher catalytic activity of SGO, an experiment was first conducted to assess the fate of carbonaceous materials during the degassing step at 100 °C under vacuum for 24 h, a prerequisite of the N_2-BET protocol. All four materials suffered a noticeable weight loss (graphene 1.2%, GO 26.0%, SGO 17.8%, and SG 13.4%) due to volatility of oxygen-bearing functional groups on graphene

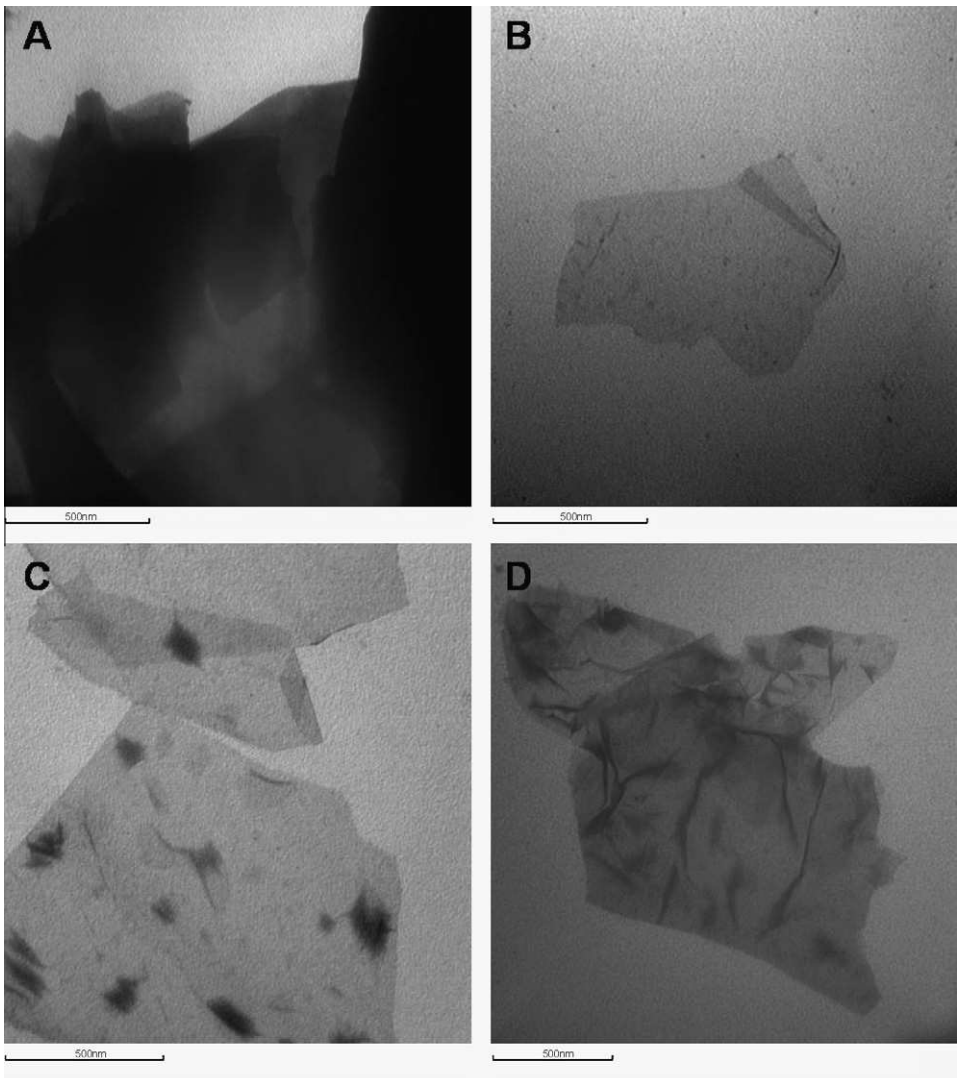

Fig. 3 – TEM images of (A) graphene, (B) GO, (C) SGO and (D) SG.

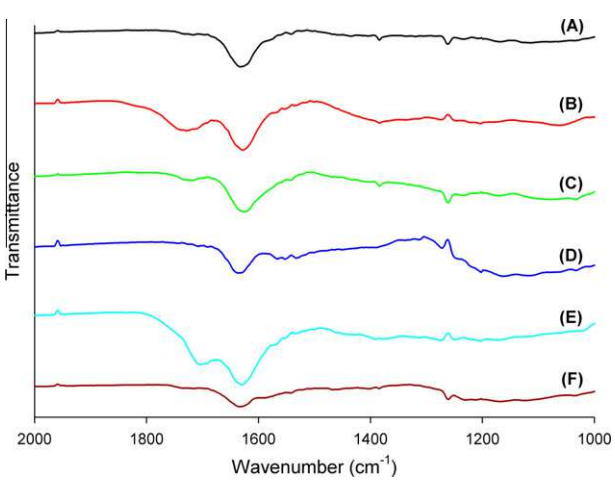

Fig. 4 – FTIR spectra of (A) graphene, (B) GO, (C) SGO, (D) SG, (E) SGO after 12 runs, and (F) 200 °C water treated SGO.

surface. Hence, surface area values were obtained by measuring the adsorption of 1-naphthol (Table 1), a technique known to give a comparable value obtained by N_2-BET for sulfonated graphene (590 m^2/g vs 520 m^2/g) [23]. Strong π–π interactions exist through face-to-face stacking between the graphene sheet and the aromatic 1-naphthol molecule [35]. Considering each 1-naphthol molecule occupies 0.43 nm^2, commercial graphene nanoplatelets used in this study had a surface area of 128 m^2/g vs 100 m^2/g as specified by the supplier. The determined surface area of GO, SGO, and SG was 318 m^2/g, 680 m^2/g and 634 m^2/g, respectively compared to 2600 m^2/g for the theoretical specific area of graphene [36]. The value obtained for SG was in good agreement with that of 590 m^2/g reported by Hu and co-workers [23]. Hence, the higher catalytic activity of SGO was likely attributed to other factors since SGO and SG had a similar surface area. GO and SG also gave similar furfural yields, yet GO had only half the surface area of SG. It should be noted that for solid acid catalysts in furfural production, the quantity and type of acidic groups, rather than surface area, were the major contributing factors to obtaining higher furfural yields [7,37–39].

SGO was selected for further studies due to its higher activity and anticipated stability at high reaction

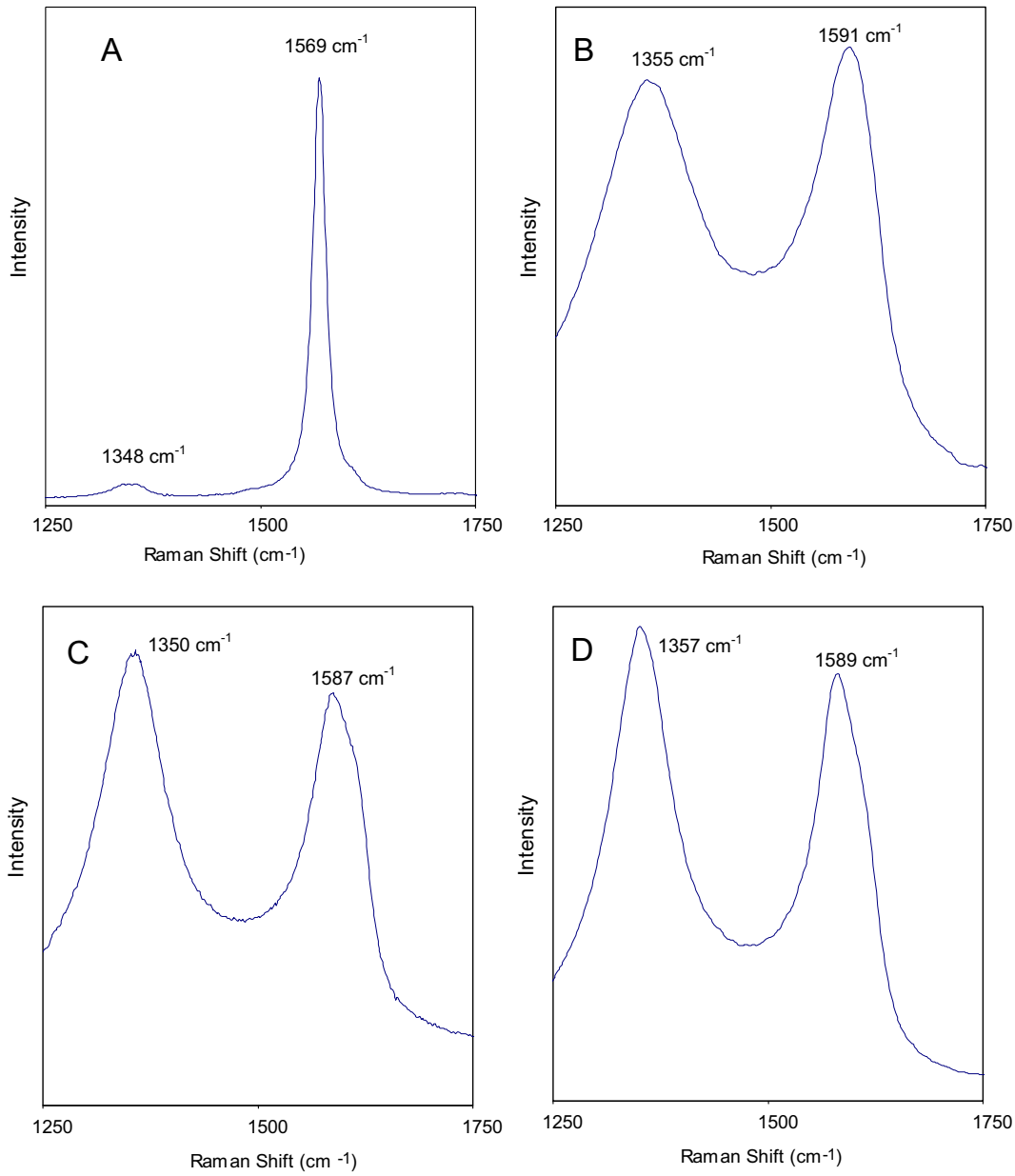

Fig. 5 – Raman spectra of (A) graphene, (B) GO, (C) SGO and (D) SG.

temperatures expected for efficient aqueous xylose conversion. As SGO catalyst loading increased from 0.5 wt.% to 5 wt.% vs xylose, a maximum yield of 66% was achieved for 0.5 wt.% loading in 35 min (Fig. 8A). Sufficient catalytic sites as low as 0.5 wt.% loading were available for the xylose dehydration in the experimental system (xylose:H^+ ratio = 784:1). It should be noted that in some situations where liquid mineral acids are used, there are greater than stoichiometric amounts of protons, resulting in the use of large amounts of acids that adds to the cost of handling and neutralization prior to product recovery and waste disposal [2,13]. Apart from minimizing catalyst and operational costs, lower catalyst loadings may also be effective in reducing product loss from humin formation, as seen by the drop in yield when the catalyst loading was greater than 0.5 wt.%.

Fig. 8B shows the effects of temperature for the production of furfural with and without catalyst. Peak furfural yields of only 1% and 12% were obtained at 150 °C and 175 °C, respectively. At 200 °C, a clear difference in furfural yield was achieved between the uncatalyzed and 0.5 wt.% loading catalyst scenarios. Unfortunately, the increase in yield when using the catalyst was non-existent at lower temperatures. After 40 min at 200 °C the yield began to drop, likely because the competing side reactions of humin formation became more pronounced with increased residence time of the product in the reactor.

To test its reusability, the catalyst was removed from the reaction mixture by filtration and dried to remove water and soluble impurities. The isolated catalyst was used directly in the next run by adding the same amount of starting water and xylose as the initial run. After 12 consecutive runs, SGO

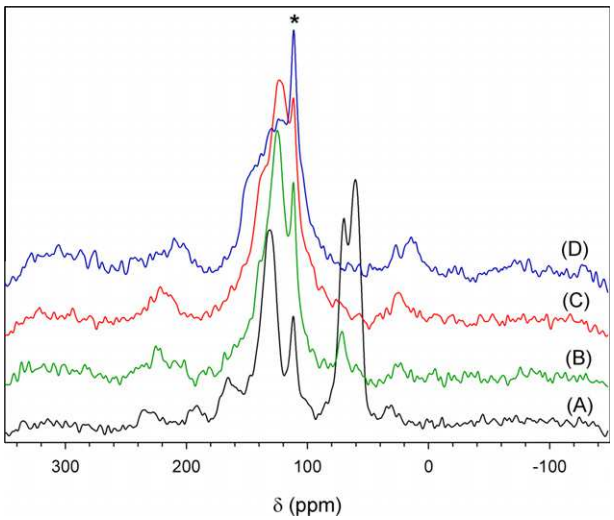

Fig. 6 – ^{13}C MAS NMR spectra of (A) GO, (B) SGO, (C) SG and (D) used SGO (* at 112 ppm corresponds to Teflon components of the NMR probe).

Table 2 – XPS elemental composition data for graphene derivatives.

Catalyst	C	O	S	Other elements
GO	60.9	36.2	1.7	1.2
SGO	75.2	19.9	1.8	3.1
SG	82.3	13.2	2.0	2.5

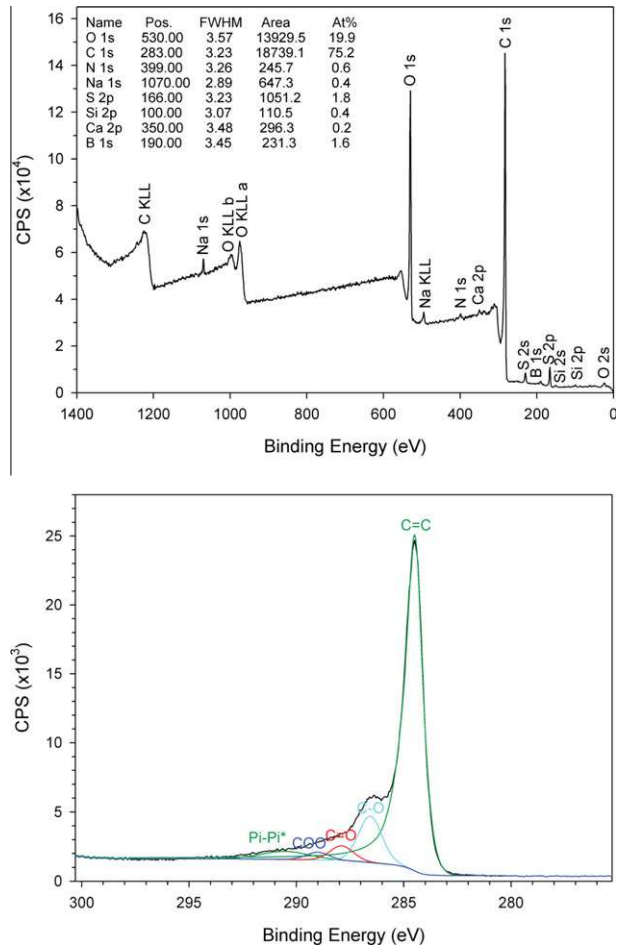

Fig. 7 – XPS spectrum of SGO (top); high resolution XPS spectrum of the C 1s peak with relative contents: C=C (82.0%), C–O (12.1%), C=O (3.9%), C(O)O (2.0%) (bottom).

still provided an average furfural yield of 61%, with individual runs ranging from 57% to 66% (Fig. 8C).

The used SGO catalyst had the appearance of micro-sized spheres in the SEM image (Fig. 9, left), but in the TEM image (Fig. 9, right), its sheet-like appearance remained unchanged. The FTIR (Fig. 4E) and ^{13}C MAS NMR (Fig. 6D) spectrum of the used catalyst did not show the peaks associated with furfural while characteristic peaks for aryl SO_3H functional groups of pristine SGO were retained (Figs. 4 and 6). The Raman spectrum (Fig. 10, left) of the used catalyst showed bands at 1354 cm^{-1} and 1589 cm^{-1} with a I_D/I_G ratio of 1.37. The elemental mass ratios of carbon, oxygen and sulfur for used SGO were 83.8%, 16.1% and 0.1%, respectively. Accumulation of organic impurities absorbed on the surface of the catalyst would account for the increase in carbon content and the decrease in sulfur content. This is consistent with the additional peaks in the carbonyl stretching region of the IR spectrum and the ^{13}C MAS NMR (>200 ppm), as well as the increased I_D/I_G ratio of 1.37 in the Raman spectrum, likely attributed to the presence of carbonaceous byproducts such as humins with carbonyl groups on the surface of the catalyst [40].

TGA was performed on different graphene and its derivatives (Fig. 11); some of the mass losses observed below 200 °C could be attributed to desorption of water or other volatiles. As expected, graphene has very high thermal stability with a $T_{95\%}$ of 523 °C. The addition of functional groups reduced the material's thermal stability, as seen in the greatly lowered $T_{95\%}$ of 161 °C for GO that has oxygen-bearing groups that are easily lost [41]. SG is more stable than SGO, with $T_{95\%}$ values of 226 °C and 152 °C, respectively, as SG has significantly fewer COOH or OH groups due to the hydrazine reduction process. For the used SGO catalyst, at temperatures over 300 °C, significant mass loss was observed in comparison to the pristine SGO, consistent with the decomposition of carbonaceous humin materials accumulated on the catalyst surface [7]. However, these impurities did not result in any significant activity decrease (Fig. 8C). Although the TGA spectrum for SGO clearly showed thermal degradation by 200 °C, potentially due to the loss of COOH groups, the active acidic sites for dehydration of xylose to furfural are the more thermally stable SO_3H groups since there was no loss in activity in the reusability studies [42]. The loss of labile oxygen-bearing groups such as COOH and OH is corroborated by the lowered IEC value of 0.75 meq H^+/g and an increase in thermal stability observed for the used SGO catalyst ($T_{95\%}$ of 206 °C).

To confirm this hypothesis, pristine SGO was heated to 200 °C in water for 5 h and isolated. The FTIR (Fig. 4F) and EDX elemental analysis of the isolated graphene material confirmed the retention of its aryl SO_3H functional groups. The lowered I_D/I_G ratio of 1.07 in its Raman spectrum

Table 3 – Dehydration of xylose in water for the production of furfural.[a]

Entry	Catalyst	Conversion (%)	Selectivity (%)	Yield (%)
1	None	76	58	44
2	Graphene	75	68	51
3	GO	80	66	53
4	SGO	83	75	62
5	SG	86	64	55

[a] Time: 35 min, temp: 200 °C, catalyst loading: 2 wt.%. Data averaged over 3 runs.

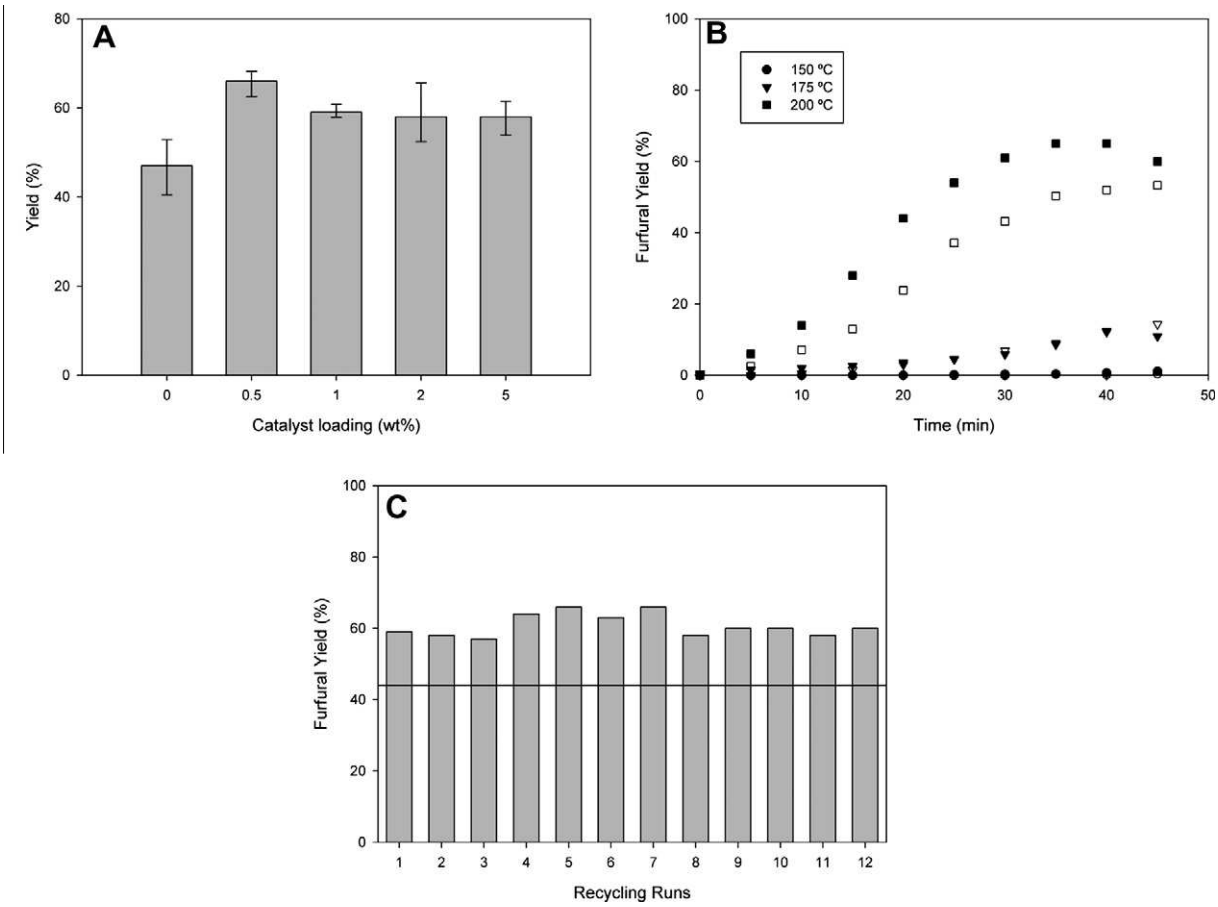

Fig. 8 – (A) Effect of the catalyst loading on the furfural yield for three runs, error bars represent 95% confidence intervals (3% xylose in water, 200 °C, 35 min). (B) Effect of temperature on catalyst activity (closed points represent 0.5% SGO wt. loading vs xylose, open points represent no catalyst). (C) Furfural yield from recycling SGO (0.5 wt.% loading vs xylose, 200 °C, 35 min); the horizontal line denotes 44% furfural yield for the non-catalyzed reaction.

(Fig. 10, right) is consistent with the removal of oxygen-bearing functional groups from the graphene surface. This is similar to the reduction of SGO to SG in which the I_D/I_G value decreases from 1.27 to 0.78. The water treated SGO sample retained its catalytic activity as well, achieving a 63% furfural yield at 200 °C in 30 min using a 0.5 wt.% catalyst loading vs xylose. No sulfur was detected in the evaporated residue of the aqueous phase by EDX, confirming the stability of the catalyst. The measured IEC value of 0.76 meq H^+/g for this water pre-treated catalyst was almost identical to that of the used SGO isolated after multiple reuses and was similar to SG, confirming the loss of oxygen-bearing groups and the retention of SO_3H groups upon heating to 200 °C.

Oxygen-bearing groups are not stable at 200 °C and are likely lost over the course of the twelve catalyst reusability runs, while the aryl SO_3H groups remain intact. However, there is no yield decrease associated with the loss of the COOH groups, suggesting that the catalytically active groups in SGO are the SO_3H groups, due to their greater acid strength and stability. The conversion of SGO to SG results in the reduction of COOH groups as well as the removal of some SO_3H groups [21], reducing the number of catalytically active sites. Conversely, removing COOH groups by thermal degradation preserves all of the SO_3H groups, which accounts for the used SGO being more catalytically active than SG.

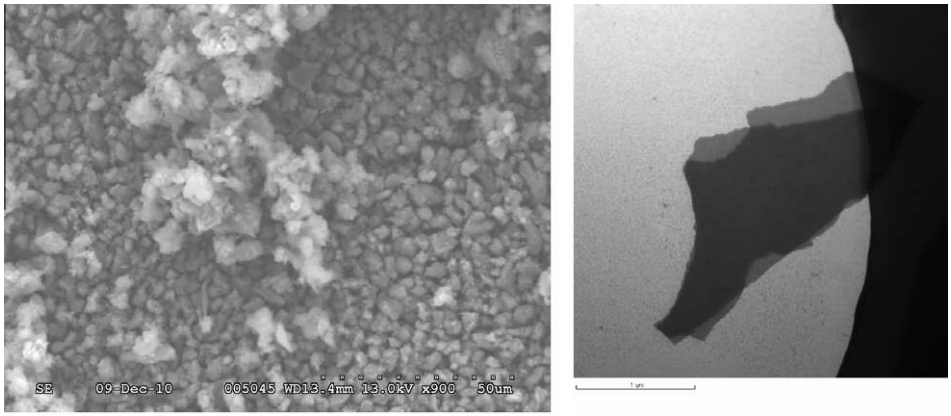

Fig. 9 – SEM (left) and TEM (right) images of a typical used SGO material after 12 consecutive runs.

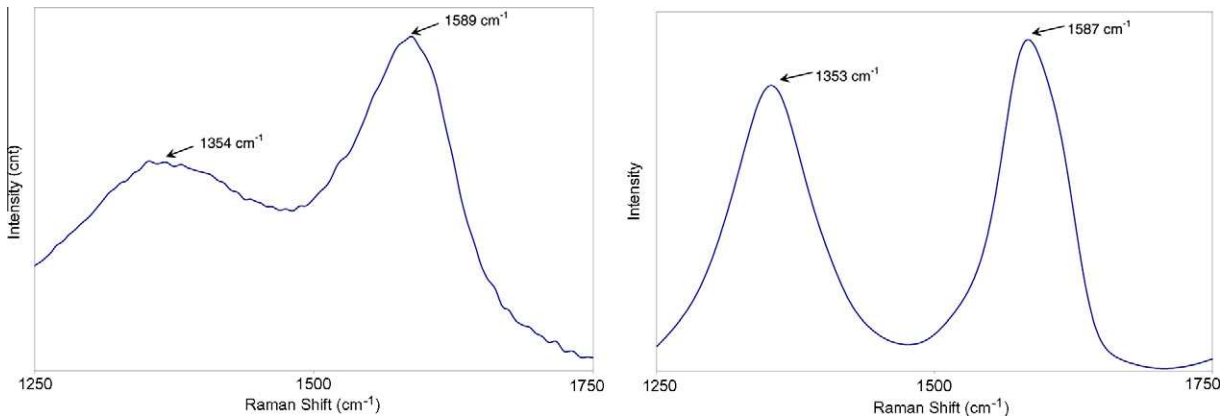

Fig. 10 – Raman spectra of a typical used SGO material after 12 consecutive runs (left) and SGO treated in water at 200 °C for 5 h (right).

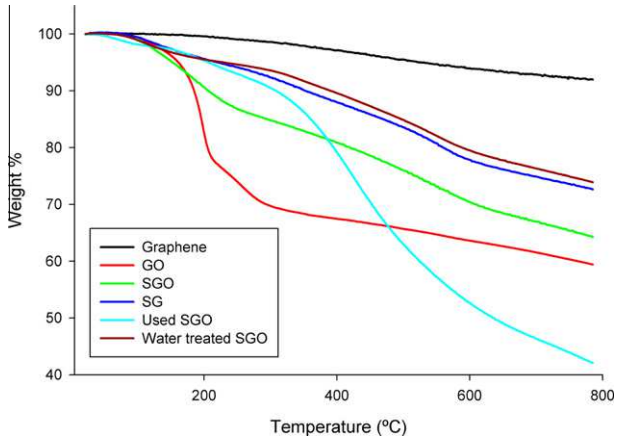

Fig. 11 – Thermogravimetric analysis of graphene and its derivatives.

4. Conclusions

In summary, we have described the use of sulfonated graphene oxide (SGO) as an active and stable catalyst for improving the yield of furfural production in aqueous xylose solutions. At only 0.5 wt.% loading vs xylose, its reusability has been demonstrated, maintaining an average yield of 61% and stability over multiple runs despite the presence of accumulated byproducts on the catalyst surface. A significant yield and short reaction time were achieved at a low catalyst loading in comparison to the uncatalyzed system and the use of conventional liquid and solid acid catalysts. This SGO catalyst takes advantage of excellent thermal and mechanical properties associated with carbon materials [43,44]. The strongly acidic aryl SO_3H groups are responsible for the catalytic activity, and the high stability of the C–C bond anchoring these groups to the conjugated graphene sheet enables the catalyst to remain active after repeated reactions at 200 °C, i.e., an ideal temperature for rapid conversion of xylose to furfural. It is desirable to increase the SO_3H substitution of the materials to generate a more active catalyst. This is another example of how low cost, reusable carbocatalysts can be used to promote reactions that convert biomass to sustainable chemical building blocks [15,16]. Doubtlessly, the use of SGO as a carbocatalyst can be extended to other important organic reactions [45] as exemplified by its reusability in the hydrolysis of ethyl acetate with comparable activity to H_2SO_4 [18].

REFERENCES

[1] Corma A, Iborra S, Velty A. Chemical routes for the transformation of biomass into chemicals. Chem Rev 2007;107:2411–502.
[2] Xing R, Subrahmanyam AV, Olcay H, Qi W, van Walsum GP, Pendse H, et al. Production of jet and diesel fuel range alkanes from waste hemicellulose-derived aqueous solutions. Green Chem 2010;12:1932–46.
[3] Moreau C, Durand R, Peyron D, Duhamet J, Rivalier P. Selective preparation of furfural from xylose over microporous solid acid catalysts. Ind Crop Prod 1998;7: 95–9.
[4] Lima S, Pillinger M, Valente AA. Dehydration of D-xylose into furfural catalysed by solid acids derived from the layer zeolite Nu-6(1). Catal Comm 2008;9:2144–8.
[5] O'Neill R, Ahmad MN, Vanoye L, Aiouache F. Kinetics of aqueous phase dehydration of xylose into furfural catalyzed by ZSM-5 zeolite. Ind Eng Chem Res 2009;48:4300–6.
[6] Dias AS, Pillinger M, Valente AA. Liquid phase dehydration of D-xylose in the presence of Keggin-type heteropolyacids. Appl Catal A 2005;285:126–31.
[7] Dias AS, Pillinger M, Valente AA. Dehydration of xylose into furfural over micro-mesoporous sulfonic acid catalysts. J Catal 2005;229:414–23.
[8] Mauritz KA, Moore RB. State of understanding of Nafion. Chem Rev 2004;104:4535–85.
[9] Lam E, Majid E, Leung ACW, Chong JH, Mahmoud KA, Luong JHT. Synthesis of furfural from xylose by heterogeneous and reusable Nafion catalysts. Chem Sus Chem 2011;4:535–41.
[10] Okuhara T. Water-tolerant solid acid catalysts. Chem Rev 2002;102:3641–66.
[11] Oefner PJ, Lanziner AH, Bonn G, Bobleter O. Quantitative studies on furfural and organic acid formation during hydrothermal, acidic and alkaline degradation of D-xylose. Monatsh Chem 1992;123:547–56.
[12] Lamminpää K, Tanskanen J, Study of furfural formation using formic acid. In: Proceedings of the 8th world congress of chemical engineering, 2009 August 23–27, Montreal, Canada.
[13] Marcotullio G, De Jong W. Chloride ions enhance furfural formation from D-xylose in dilute aqueous acidic solutions. Green Chem 2010;12:1739–46.
[14] Smuk JM, Zoch LL, Furfural yield and decomposition in sodium 2,4-dimethylbenzenesulfonate–sulfuric acid–water solutions, Report no.: FPL32. Forest Service, Madison (WI): USA; 1965 June. 8p.
[15] Toda M, Takagaki A, Okamura M, Kondo JN, Hayashi S, Domen K, et al. Green chemistry: biodiesel made with sugar catalyst. Nature 2005;438:178.
[16] Wang J, Xu W, Ren J, Liu X, Lu G, Wang Y, Efficient catalytic conversion of fructose into hydroxymethyl furfural by a novel carbon-based solid acid. Green Chem. doi:10.1039/c1gc15306d.
[17] Zhang B, Ren J, Liu X, Guo Y, Lu G, Wang Y. Novel sulfonated carbonaceous materials from *p*-toluenesulfonic acid/glucose as a high-performance solid-acid catalyst. Catal Commun 2010;11:629–32.
[18] Ji J, Zhang G, Chen H, Wang S, Zhang G, Zhang F, et al. Sulfonated graphene as water-tolerant solid acid catalyst. Chem Sci 2011;2:484–7.
[19] Hummers WS, Offeman RE. Preparation of graphitic oxide. J Am Chem Soc 1958;80:1339.
[20] Kovtyukhova NI, Ollivier PJ, Martin BR, Mallouk TE, Chizhik SA, Buzaneva EV, et al. Layer-by-layer assembly of ultrathin composite films from micron-sized graphite oxide sheets and polycations. Chem Mater 1999;11:771–8.
[21] Si Y, Samulski ET. Synthesis of water soluble graphene. Nano Lett 2008;8:1679–82.
[22] López DE, Goodwin Jr JG, Bruce DA. Transesterification of triacetin with methanol on Nafion® acid resins. J Catal 2007;245:381–91.
[23] Zhao G, Jiang L, He Y, Li J, Dong H, Wang X, et al. Sulfonated graphene for persistent aromatic pollutant management. Adv Mater 2011;23:3959–63.
[24] Haber J. Manual on catalyst characterization. Pure Appl Chem 1991;63:1227–46.
[25] He H, Klinowski J, Forster M, Lerf A. A new structural model for graphite oxide. Chem Phys Lett 1998;287:53–6.
[26] Lerf A, He H, Forster M, Klinowski J. Structure of graphite oxide revisited. J Phys Chem B 1998;102:4477–82.
[27] Stankovich S, Piner RD, Nguyen ST, Ruoff RS. Synthesis and exfoliation of isocyanate-treated graphene oxide nanoplatelets. Carbon 2006;44:3342–7.
[28] Ferrari AC, Meyer JC, Scardeli V, Casiraghi C, Lazzeri M, Mauri F, et al. Raman spectrum of graphene and graphene layers. Phys Rev Lett 2006;97:187401-1–4.
[29] Lazzeri M, Mauri F. Nonadiabatic Kohn anomaly in a doped graphene monolayer. Phys Rev Lett 2006;97:266407-1–4.
[30] Cai W, Piner RD, Stadermann FJ, Park S, Shaibat MA, Ishii Y, et al. Synthesis and solid-state NMR structural characterization of ^{13}C-labeled graphite oxide. Science 2008;321:1815–7.
[31] Hontoria-Lucas C, Lopez-Peinado AJ, Lopez-Gonzalez JDD, Rojas-Cervantes ML, Martin-Aranda RM. Study of oxygen-containing groups in a series of graphite oxides: physical and chemical characterization. Carbon 1995;33:1585–92.
[32] Titelman GI, Gelman V, Bron S, Khalfin RL, Cohen Y, Bianco-Peled H. Characteristics and microstructure of aqueous colloidal dispersions of graphite oxide. Carbon 2005;43:641–9.
[33] Stankovich S, Dikin DA, Dommett GHB, Kohlhaas KM, Kleinhammes A, Jia Y, et al. Synthesis of graphene-based nanosheets via chemical reduction of exfoliated graphite oxide. Carbon 2007;45:1558–65.
[34] Akiya N, Savage PE. Roles of water for chemical reactions in high-temperature water. Chem Rev 2002;102:2725–50.
[35] Zhao G, Li J, Wang X. Kinetic and thermodynamic study of 1-naphthol adsorption from aqueous solution to sulfonated graphene nanosheets. Chem Eng J 2011;173:185–90.
[36] Stankovich S, Dikin DA, Piner RD, Kohlhaas KM, Zimney EJ, Stach EA, et al. Graphene-based composite materials. Nature 2006;442:282–6.
[37] Dias AS, Pillinger M, Valente AA. Mesoporous silica-supported 12-tungstophosphoric acid catalysts for the liquid phase dehydration of D-xylose. Micropor Mesopor Mater 2006;94:214–25.
[38] Dias AS, Lima S, Brandão P, Pillinger M, Rocha J, Valente AA. Liquid-phase dehyration of D-x-xylose over microporous and mesoporous niobium silicates. Catal Lett 2006;108:179–86.
[39] Weingarten R, Tompsett GA, Conner Jr WC, Huber GW. Design of solid acid catalysts for aqueous-phase dehydration of carbohydrates: the role of Lewis and Bronsted acid sites. J Catal 2011;279:174–82.
[40] Gandini A, Belgacem MN. Furans in polymer chemistry. Prog Polym Sci 1997;22:1203–379.
[41] Wang G, Yang J, Park J, Gou X, Wang B, Liu H, et al. Facile synthesis and characterization of graphene nanosheets. J Phys Chem C 2008;112:8192–5.
[42] Bekyarova E, Itkis ME, Ramesh P, Berger C, Sprinkle M, de Heer WA, et al. Chemical modification of epitaxial graphene: spontaneous grafting of aryl groups. J Am Chem Soc 2009;131:1336–7.
[43] Hara M, Yoshida T, Takagaki A, Takata T, Kondo JN, Hayashi S, et al. A carbon material as a strong protonic acid. Angew Chem Int Ed 2004;43:2955–8.

[44] Wang XQ, Liu R, Waje MM, Chen ZW, Yan YS, Bozhilov KN, et al. Sulfonated ordered mesoporous carbon as a stable and highly active protonic acid catalyst. Chem Mater 2007;19:2395–7.

[45] Dreyer DR, Jia H-P, Bielawski CW. Graphene oxide: a convenient carbocatalyst for facilitating oxidation and hydration reactions. Angew Chem Int Ed 2010;49:6813–6.